Available online at www.sciencedirect.com
SCIENCE DIRECT
C. R. Biologies 328 (2005) 1073–1082
COMPTES RENDUS BIOLOGIES
http://france.elsevier.com/direct/CRASS3/

Biophysics / Biophysics

Dissociation of nuclear import cargo complexes by the protein Ran: a fluorescence correlation spectroscopy study

Cécile Fradin [a,*], David Zbaida [b], Michael Elbaum [b]

[a] *Department of Physics and Astronomy and Department of Biochemistry and Biomedical Sciences, 1280 Main St. W, Hamilton, ON, L8S4M1, Canada*

[b] *Department of Materials and Interfaces, Weizmann Institute of Sciences, Rehovot 76100, Israel*

Received 31 May 2005; accepted after revision 3 October 2005

Available online 2 November 2005

Presented in the framework of the European Workshop on Fluorescence Correlation – Spectroscopy Techniques Applications in Biology, Medicine and Pharmacology, Faculty of Medicine of Paris-Sud, Le Kremlin-Bicêtre, France, 24 & 25 March 2005

Presented by Jean Rosa

Abstract

In nucleated cells, proteins designed for nuclear import form complexes with soluble nuclear transport receptors prior to translocation across the nuclear envelope. The directionality of transport is due to the asymmetric distribution of the protein Ran, which dissociates import cargo complexes only in its nuclear RanGTP form. Using fluorescence correlation spectroscopy, we have studied the stability of cargo complexes in solution in the presence and in the absence of RanGTP. We find that RanGTP has a higher affinity for the major import receptor, the importin α/β heterodimer, when importin α does not carry a cargo, suggesting that some nuclear transport targets might be preferentially released. ***To cite this article: C. Fradin et al., C. R. Biologies 328 (2005).***

Résumé

Dissociation du complexe importin α/importin β par la protéine Ran : une étude par corrélation de fluorescence. Les protéines destinées à être importées dans le noyau cellulaire forment avec plusieurs récepteurs solubles un complexe qui est ensuite acheminé à travers la membrane nucléaire. Dans le noyau, le complexe est dissocié par la forme nucléaire de la protéine Ran, RanGTP. La distribution asymétrique de cette protéine dans la cellule assure la directionnalité du transport. Nous avons étudié par des techniques de corrélation de fluorescence la dissociation du complexe formé autour du cargo en solution. Nous montrons que l'affinité de RanGTP pour ce complexe est dépendante de la présence du cargo. Ceci suggère que certains cargos sont relâchés en priorité. ***Pour citer cet article : C. Fradin et al., C. R. Biologies 328 (2005).***

Keywords: Nucleocytoplasmic transport; Nuclear import; Karyopherins; Importins; Nuclear localization signal; NLS; Ran; RanGTP; RanGDP; FCS

Mots-clés : Transport nucléocytoplasmique ; Import nucléaire ; Karyopherines ; Importines ; Signal de localisation nucléaire ; Ran ; RanGTP ; RanGDP ; Corrélation de fluorescence

* Corresponding author.
E-mail address: fradin@physics.mcmaster.ca (C. Fradin).

1631-0691/$ – see front matter
doi:10.1016/j.crvi.2005.10.003

1. Introduction

Nucleocytoplasmic transport is a vital process for nucleated cells, which need to regulate the flow of macromolecules transiting between the cytoplasm and the nucleus [1–4]. Molecules larger than 50 kDa are usually transported across the nuclear envelope via an active process able to pump macromolecules against a concentration gradient. Both nuclear import and export take place through the large nuclear pore complexes spanning the nuclear membrane. However, a different set of soluble receptors is required in each case. In animal cells, the main import pathway involves the two soluble receptors importin α and importin β. These bind to import cargoes carrying short amino acid sequences known as nuclear localization signals (NLSs), forming a heterotrimer called the cargo complex. This complex is subsequently able to find its way to the nuclear envelope and through a nuclear pore complex. The translocation is facilitated by the interaction of importin β with protein components of the nuclear pore containing phenylalanine–glycine repeats.

Once in the nucleus, the cargo complex is dissociated by the GTP-binding protein Ran, which in its nuclear Ran-GTP form binds importin β with high affinity [5]. After cargo release, the Ran/importin β complex is transported back to the cytoplasm, where the cytoplasmic protein RanBP1 catalyzes the hydrolysis of RanGTP into RanGDP. This causes Ran to change conformation, leading to the release of importin β in the cytoplasm. Importin α is also actively re-exported back to the cytoplasm, after forming a complex with the soluble export factor CAS and RanGTP. The transported cargo, on the other hand, remains in the nucleus, free to carry out its nuclear function but unable to traverse the nuclear pore in the other direction. The cycle is completed with RanGDP being returned to the nucleus via association with the soluble import factor NTF2, and there is an undergoing nucleotide exchange for GTP supported by the chromatin associated protein RCC1. This permits the restoration of the nuclear pool of RanGTP. Indeed, the different interactions of Ran with the numerous Ran-binding proteins present in the cytoplasm and in the nucleus result in a primarily nuclear localization of the protein during interphase, as well as in an asymmetric distribution of the two different forms of Ran: the predominant form of Ran in the nucleus is RanGTP, while the predominant form of Ran in the cytoplasm is RanGDP [6]. This RanGTP to RanGDP gradient across the nuclear membrane thus ultimately drives vectorial nuclear transport.

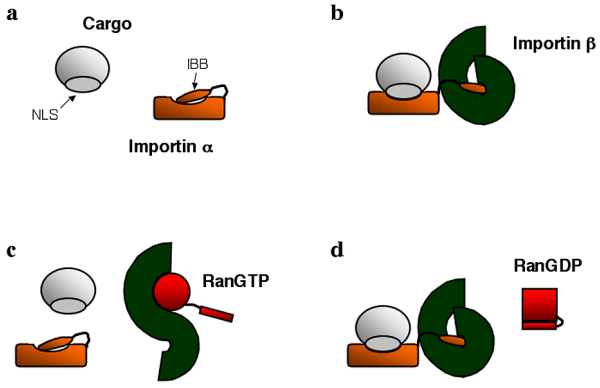

Fig. 1. Schematic representation of various soluble factors involved in nuclear import: import cargo carrying a nuclear localization signal (NLS), importin α with its importin β binding domain (IBB), importin β, RanGTP and RanGDP. Panels (**a**), (**b**), (**c**) and (**d**) highlight the possible interactions among these proteins.

Interestingly, the same set of soluble factors that are involved in nuclear import have been shown to intervene in a number of other different cellular processes [7]. During mitosis, the importin α/β complex inhibits spindle assembly factors by binding to them, while RanGTP, by releasing these factors from the α/β complex, promotes spindle assembly [8,9]. It has also been proposed that RanGTP, which is expected to remain associated with chromatin during interphase, may control other chromatin related processes, for example, the assembly of the nuclear membrane around the chromatin as well as assembly of the nuclear pore complexes [10,11]. In addition, recent evidence links Ran and importin β to the control of the duplication of the microtubule organizing center [12]. Finally, RanGTP and importin β seem to have a connection to gene transcription, since the former is found associated with transcriptionally inactive and the latter with transcriptionally active genes on the chromatin [13]. A common theme in many of these cellular processes could be the capacity of RanGTP to act as a molecular switch by turning on or off the interactions between the importin α/β heterodimer and different key targets.

This molecular switch capacity is enabled by the clever pattern of interactions existing between nuclear localization signals, importin α, importin β and Ran. These interactions (summarized in Fig. 1) have been understood through a series of structural and biochemical studies [14–18]. The recognition of a NLS by importin α occurs only in presence of importin β. This is because importin α itself carries at its N terminus an auto-inhibitory NLS-like domain rich in basic amino acids, which competes with the binding of other NLSs to the protein (Fig. 1a) [16]. This auto-inhibitory do-

main is also the importin β binding (IBB) motif of importin α. As a result, when importin β binds importin α, it sequesters the auto-inhibitory domain, exposing the NLS binding groove and allowing NLS-carrying proteins to interact with importin α (Fig. 1b). On the other hand, the binding of RanGTP to importin β competes with the binding of importin β with importin α, since on importin β the binding domains for importin α and RanGTP partially overlap. So the effect of RanGTP is to release the cargo from the importin α/β complex. Its binding to importin β releases the auto-inhibitory domain of importin α, which in turn detaches from the NLS carrying protein cargo (Fig. 1c). Most importantly, only RanGTP, and not RanGDP, can bind to importin β. This is because the importin β binding domain of Ran is only accessible when Ran is bound to GTP (Fig. 1d).

In this article, we report our efforts to apply fluorescence correlation spectroscopy (FCS) [19–22] to the study of the formation and dissociation of transport cargoes. These experiments were carried out *in vitro* with purified proteins and fluorescently labeled peptides carrying an NLS sequence. The advantage of using FCS over other techniques, for example, plate-based biosensors, is that the actual solution interactions of the proteins are probed. Our study confirms that NLS carrying peptides and importin α can bind, but only in the presence of importin β, and only when the peptide carries the correct NLS sequence. It also confirms that RanGTP, but not RanGDP, is able to dissociate the cargo complex. In addition, we show that RanGTP binds preferentially to importin α/importin β complexes that do not carry a transport cargo. This finding raises the interesting question of whether importin β complexes may be dissociated preferentially by RanGTP according to their target.

2. Materials and methods

2.1. Fluorescent peptides

The sequences of the two peptides used in this study were CTPPKKKRKV and CTPVKRKKKP. The first peptide, referred to as NLS peptide in the following, contains the nuclear localization signal corresponding to residues 126–132 on the SV40 large T-antigen, PKKKRKV. This NLS is connected to a C-terminal cysteine by a linker sequence, TP. The second peptide, referred to as bNLS peptide in the following, is similar to the first one, except for the fact that the NLS sequence has been inverted. As a result, both peptides have the same overall electrostatic properties, but only the first one contains the proper amino acid sequence for identification as an import cargo. Both peptides were synthesized in the lab of Dr. Mati Fridkin, and purified by preparative thin-layer chromatography. MALDI-TOF mass spectrometry showed that the purified peptides had the expected 1.18-kDa molecular weight. They were subsequently linked to an Alexa dye (Alexa Fluor 546 C_5 maleimide, Molecular Probes) through maleimide chemistry. Briefly, 0.6 mM of peptide was allowed to react with a 1.3-fold excess of Alexa dye in a phosphate buffer (NaH_2PO_4, 50 mM, pH = 7.1, adjusted with NaOH) for 2 h at room temperature and then overnight at 4 °C, while rotating the solution end-to-end continuously. The crude reaction mixture was purified in a size exclusion column (P-2 Bio-Gel, from Bio-Rad) with an exclusion limit of 1.8 kDa. The reaction mixture was eluted with ammonium hydrogen carbonate (0.1 M) at 4 °C. The collected fractions were analyzed by thin-layer chromatography. The product was lyophilized and re-dissolved in water twice to remove salt. Analysis by mass-spectrometry confirmed that the product had the expected 2.2-kDa molecular weight.

2.2. Purified proteins

Purified human importin α and human importin β were a kind gift of Dr. Dirk Görlich. Purified RanQ69L was a kind gift of Dr. Renat Nevo. RanQ69L is a mutant of human Ran, which inhibits GTP hydrolysis [23]. RanQ69L-GTP is very unlikely to hydrolyze into RanQ69L-GDP. The method used for loading the protein with either GDP or GTP is described in detail in [24]. The purity of all proteins was checked by SDS–PAGE, and the concentrations of the stock solutions were measured by absorption at 280 nm. All the titrations presented here were carried out in PBS buffer (pH = 7.4) containing 0.1% digitonin and 5 $g l^{-1}$ ovalbumin (both purchased from Sigma). The ovalbumin was added in order to prevent adsorption on the microscope coverslips used for the FCS experiments (cf. § *Results*).

2.3. Fluorescence correlation spectroscopy

A home-built apparatus, described elsewhere [25], was used to perform FCS experiments. Briefly, fluorescence was excited by a 543.5-nm He–Ne laser focused in the sample by an oil objective (Zeiss, Achrostigmat, 100×/1.25). The intensity of the laser beam was controlled by a pair of polarizers, resulting in a radiant exposure at the focus on the order of 10 $\mu W\,\mu m^{-2}$. Fluorescence emission was collected through the same objective, focused through a 50-μm pinhole, and detected by a photon counting head (H7421, Hamamatsu). The

signal obtained was autocorrelated on-line by a hardware correlator (Flex 99R-12D, correlator.com). The sample chamber was constructed from a standard glass microscope slide, covered by parafilm gently heated to adhere. On this parafilm layer, which was introduced to prevent protein adsorption on the glass slide two parafilm bands were placed about 2 mm apart, and covered by a microscope coverslip of thickness 0.17 mm. The chamber was then gently heated again to allow for the different parts to adhere. The solution was introduced from the side of the chamber, after which the sample was sealed with wax. The volume of the solutions in the samples was 5 µl. To avoid optical aberrations due to index mismatch between the oil and the aqueous sample, measurements were taken only 10 µm away from the coverslip. All measurements were made at room temperature. All titrations were repeated at least twice, and for each titration, each point is the average of at least two FCS measurements. All curves were analyzed using Kaleidagraph.

Before each experiment, the detection volume was first calibrated using the diffusion of Rhodamine 610, purchased from Exciton. The autocorrelation curves obtained from diffusion of the dye were analyzed using the expression [26]:

$$G(t) = \frac{1}{\langle N\rangle}\frac{1}{(1+t/\tau_{\mathrm{D}})\sqrt{1+t/S^2\tau_{\mathrm{D}}}} \times\left(1+\frac{T}{1-T}\mathrm{e}^{-t/\tau_{\mathrm{T}}}\right) \tag{1}$$

which takes into account the diffusion of the molecules through the detection volume and the existence of a non-fluorescent triplet state. The residence time τ_{D} is the average time spent by the fluorescent particles in the detection volume. The $1/\mathrm{e}^2$ radius of the detection volume, w_0, can be calculated using the relationship $w_0^2 = \tau_{\mathrm{D}}/4\,D$, where D is the diffusion coefficient of the dye. In the case of Rhodamine 6G, $D = 280\ \mu\mathrm{m}^2\,\mathrm{s}^{-1}$ [27]. Since Rhodamine 610 has the same molecular weight as Rhodamine 6G, 479 $\mathrm{g\,mol}^{-1}$, we assumed that it also had the same diffusion coefficient. The aspect ratio S characterizes the geometry of the detection volume $S = z_0/w_0$, where z_0 is the $1/\mathrm{e}^2$ half-height of the revolution ellipsoid. The total volume of the detection volume can be estimated from this calibration and was found in our case to be 0.5 fl. Knowing this volume, absolute concentration of dye molecules can be calculated from $\langle N\rangle$, the number of dye molecules present on average in the detection volume. T is the fraction of the dye found in the triplet state, and τ_{T} is the associated relaxation time.

Eq. (1) was also used to account for the autocorrelation curves obtained from the diffusion of the peptides in the absence of the soluble transport factors importin α and importin β. On the contrary, the autocorrelation curves obtained from the diffusion of the peptides in presence of the transport factors were analyzed assuming a two-component model accounting for the presence of cargo complexes [28]:

$$G(t) = \frac{1}{\langle P\rangle}\left[\frac{1-y}{(1+t/\tau_{\mathrm{D},1})\sqrt{1+t/S^2\tau_{\mathrm{D},1}}} + \frac{y}{(1+t/\tau_{\mathrm{D},2})\sqrt{1+t/S^2\tau_{\mathrm{D},2}}}\right] \times\left(1+\frac{T}{1-T}\mathrm{e}^{-t/\tau_{\mathrm{T}}}\right) \tag{2}$$

The first term in this expression relates to the diffusion of the unbound peptide, where $\tau_{\mathrm{D},1}$ is the average residence time of the free peptides, while the second term relates to the diffusion of the peptides when part of a cargo complex, where $\tau_{\mathrm{D},2}$ is the average residence time of the complexes in the detection volume. The parameter y is related to the fraction f of peptides that are part of a cargo complex, as well as to the molecular brightness of the free peptides, η_1, and the molecular brightness of the peptides in the cargo complex, η_2:

$$y = \frac{f\eta_2^2}{(1-f)\eta_1^2 + f\eta_2^2} \tag{3}$$

The apparent average number of fluorophores in the detection volume, $\langle P\rangle$, is related to the actual average number of fluorophores in the detection volume, $\langle N\rangle$, by:

$$\langle P\rangle = \langle N\rangle\frac{[(1-f)\eta_1 + f\eta_2]^2}{(1-f)\eta_1^2 + f\eta_2^2} \tag{4}$$

An apparent molecular brightness η can be defined as the ratio of the average fluorescence intensity by the apparent number of fluorophores $\langle P\rangle$:

$$\eta = \frac{(1-f)\eta_1^2 + f\eta_2^2}{(1-f)\eta_1 + f\eta_2} \tag{5}$$

In the special case where both species have the same molecular brightness, then $\eta = \eta_1 = \eta_2$, $y = f$ and $\langle P\rangle = \langle N\rangle$. When analyzing the curves recorded for the peptides, the aspect ratio S was fixed to the value obtained from the analysis of the curves recorded immediately before for the diffusion of Rhodamine 610 (typically $S \approx 5$). Also, mostly, when using Eq. (2), the values of $\tau_{\mathrm{D},1}$ and $\tau_{\mathrm{D},2}$ were fixed. The value of $\tau_{\mathrm{D},1}$ was determined by analyzing the autocorrelation data obtained for a solution of peptide in the absence of soluble

import factors with a one-component model (Eq. (1)). The value of $\tau_{D,2}$ was determined by analyzing the autocorrelation data obtained for the NLS peptide in presence of a large excess of importin α and β, using a two-component model (Eq. (2)) with $\tau_{D,1}$ fixed. The diffusion coefficients of the different species were obtained by comparing their residence times to that of Rhodamine 610.

2.4. Kinetic analysis

For titration curves involving the association of a receptor (typically the importin α/β heterodimer, noted AB) with a ligand (typically the NLS peptide, noted P), the reaction was described by a simple equilibrium:

$$\mathrm{P} + \mathrm{AB} \overset{K_D}{\longleftrightarrow} \mathrm{PAB}$$

characterized by the dissociation constant K_D. The concentration of each of the three reagents can be calculated by solving the system of three equations constituted by the equilibrium equation: $K_D = [P][AB]/[PAB]$, and the two conservation of matter equations: $[P]+[PAB] = c_p$ and $[AB] + [PAB] = c_{\alpha\beta}$. The fraction of peptides part of a cargo complex, $f = [PAB]/([P] + [PAB])$, is then easily expressed as a function of the total peptide concentration c_p and the total heterodimer concentration $c_{\alpha\beta}$:

$$f = \frac{K_D + c_p + c_{\alpha\beta}}{2c_p}\left(1 - \sqrt{1 - \frac{4c_p c_{\alpha\beta}}{(K_D + c_p + c_{\alpha\beta})^2}}\right) \tag{6}$$

In addition, we observed that in some cases a small fraction f_0 of the NLS peptides (ligand) did not seem to be able to bind to the α/β heterodimer (receptor), no matter how high the receptor concentration. To account for that effect, we used a modified form of Eq. (7) when analyzing our binding curves:

$$f = (1 - f_0)\frac{K_D + c_p + c_{\alpha\beta}}{2c_p} \times \left(1 - \sqrt{1 - \frac{4c_p c_{\alpha\beta}}{(K_D + c_p + c_{\alpha\beta})^2}}\right) \tag{7}$$

When studying the dissociation of the cargo complex (noted C) by Ran (either RanGTP or RanGDP, noted R), the titration curves were analyzed considering that the relevant reaction was the equilibrium binding between the complex and the protein causing its dissociation:

$$\mathrm{C} + \mathrm{R} \overset{K_D}{\longleftrightarrow} \mathrm{CR}$$

Because when we write this reaction we disregard the actual state of the complex (i.e. whether it is bound or not to a NLS), we assume that binding of Ran to the Ran binding domain of importin β does not depend on the conformation of the latter. The fraction of cargo complex not yet dissociated by Ran, $f_{\alpha\beta} = [C]/([CR] + [C])$, then obeys an equation similar to Eq. (6):

$$f_{\alpha\beta} = 1 - \frac{K_D + c_{\alpha\beta} + c_R}{2c_{\alpha\beta}} \times \left(1 - \sqrt{1 - \frac{4c_{\alpha\beta}\, c_R}{(K_D + c_{\alpha\beta} + c_R)^2}}\right) \tag{8}$$

where c_R is the total concentration of Ran in solution.

However, if there are two different types of complexes in solution (in our case importin α/β heterodimers on their own and actual cargo complexes, i.e. importin α/β heterodimers bound to a NLS peptide), noted $C_{\alpha\beta}$ and $C_{NLS\alpha\beta}$, we should consider the possibility that Ran binds with different affinities to the two complexes. If this is the case we have two coupled reaction equations:

$$\mathrm{C}_{\alpha\beta} + \mathrm{R} \overset{K_D}{\longleftrightarrow} \mathrm{C}_{\alpha\beta}\mathrm{R}$$

$$\mathrm{C}_{NLS\alpha\beta} + \mathrm{R} \overset{K_D^{NLS}}{\longleftrightarrow} \mathrm{C}_{NLS\alpha\beta}\mathrm{R}$$

If $[C_{NLS\alpha\beta}] \ll [C_{\alpha\beta}]$, then Eq. (8) still describes the dissociation of the importin α/β heterodimer, because the perturbation due to the presence of the second species is negligible. On the other hand, to find an expression for the fraction of cargo complexes that have not been dissociated, $f_{NLS\alpha\beta} = [C_{NLS\alpha\beta}]/([C_{NLS\alpha\beta}] + [C_{NLS\alpha\beta}R])$, we need to consider both equilibriums: $K_D = [C_{\alpha\beta}][R]/[C_{\alpha\beta}R]$ and $K_D^{NLS} = [C_{NLS\alpha\beta}][R]/[C_{NLS\alpha\beta}R]$. Combining these equations, we find that:

$$\begin{aligned}[C_{NLS\alpha\beta}R]/[C_{NLS\alpha\beta}] &= \left(K_D/K_D^{NLS}\right) \times [C_{\alpha\beta}R]/[C_{\alpha\beta}] \\ &= \left(K_D/K_D^{NLS}\right) \times (1 - f_{\alpha\beta})/f_{\alpha\beta}\end{aligned}$$

which leads to:

$$f_{NLS\alpha\beta} = \frac{f_{\alpha\beta}}{1 - (1 - K_D/K_D^{NLS})(1 - f_{\alpha\beta})} \tag{9}$$

3. Results

Our earliest attempts at titrating solutions of peptides with different purified proteins showed that, as the total protein concentration in the solution was increased, and although the amount of peptide per sample was kept

constant, the concentration of peptides detected in solution increased. The increase in soluble peptide concentration was indicated both by an increase in the total average intensity and by an increase in the average number $\langle N \rangle$ of fluorophores detected in the detection volume. We found that this effect was due to a strong adsorption of the peptides on the samples glass surfaces. The two peptides used contained a majority of positively charged basic groups (lysine and arginine) and one hydrophobic group (valine), which explains the very strong affinity of the molecules for the negatively charged glass surfaces of the sample. As the total protein concentration in the sample is increased to a few µM, the proteins compete with the peptides for surface adsorption, and more peptide can be found in the solution. The adsorption of the peptides on the glass was also evidenced by a time-dependent decrease of the peptide concentration detected by FCS just after the peptide solution was introduced in the experimental chamber.

To avoid as much as possible the loss of proteins and peptides to glass and polymer surfaces while handling the solutions and taking the measurements, we then supplemented the solution with ovalbumin. We tested increasing concentrations up to 50 $\mathrm{g\,l^{-1}}$ (corresponding to about 1 mM), in solutions containing 5 nM of the Alexa-NLS peptide. Autocorrelation functions were recorded for each of these samples, and using a simple diffusion model (Eq. (1)), the average number of peptide molecules in the detection volume and their diffusion coefficient were extracted (Fig. 2). The average fluorescence intensity detected from the sample increased sharply as the protein concentration reached about 1 $\mathrm{g\,l^{-1}}$, and reached a plateau around 10 $\mathrm{g\,l^{-1}}$. The FCS measurements show that this is due to an increase in the concentration of the peptides in solution (Fig. 2a) as opposed to an increase in the apparent molecular brightness of the fluorophores, which was independent of the ovalbumin concentration up to 50 $\mathrm{g\,l^{-1}}$ (data not shown). Looking at the diffusion coefficient of the peptide (Fig. 2b), one can see that below 5 $\mathrm{g\,l^{-1}}$, the ovalbumin has no detectable effect on the mobility of the peptide. But above 5 $\mathrm{g\,l^{-1}}$, the diffusion of the peptide starts to be slowed down. Consequently, we chose to work at a 5-$\mathrm{g\,l^{-1}}$ concentration of ovalbumin, in order to reduce as much as possible the adsorption of the peptide on the glass surfaces while maintaining the viscosity of a simple aqueous solution. In addition, as explained in § *Materials and methods*, we coated all the glass surfaces of the sample with parafilm, except for a very small window allowing the laser beam to enter the sample and the fluorescence emission to be collected. This increased further the concentration

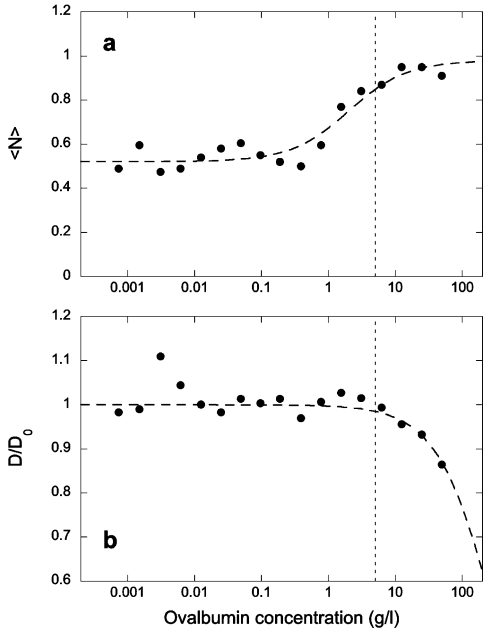

Fig. 2. (**a**) Average number of fluorescent Alexa-NLS peptides in the detection volume and (**b**) normalized diffusion coefficient of the peptide, as a function of ovalbumin concentration. All data have been obtained for a constant concentration of the peptide $c = 5$ nM introduced in the sample. Dashed lines are guide for the eyes. The vertical dotted lines indicate the concentration of ovalbumin chosen for subsequent experiments.

of peptide detected in solution. As well, we added a small quantity (0.1%) of digitonin, which also slightly improved the solubility of the peptide. The experiments shown in Fig. 2, however, were carried out in samples which were not coated with parafilm, and in the absence of digitonin.

We first measured the binding of the importin α/β heterodimer to the Alexa-NLS peptide. The α/β complex was allowed to form in an equimolar 20 µM solution of importin α and importin β. Different volumes of this solution were then mixed with a second solution containing the peptide. The final concentration of peptides in these mixed solutions was $c_p = 50$ nM, as measured by FCS. Typical autocorrelation curves, recorded at different concentration of the α/β complex, are shown in Fig. 3, as well as the corresponding fits using Eq. (2). The peptide alone was found to have a diffusion coefficient $D_1 = 140 \pm 20$ $\mu\mathrm{m^2\,s^{-1}}$, while for the complex $D_2 = 42 \pm 10$ $\mu\mathrm{m^2\,s^{-1}}$. As more proteins were added in solution, the fraction of peptides that were part of a cargo complex progressively increased, showing that binding of the NLS-peptide and the α/β heterodimer indeed occurred (Fig. 4a). The apparent molecular brightness (Eq. (4)) was calculated (Fig. 4b), and found to be independent of importin concentration.

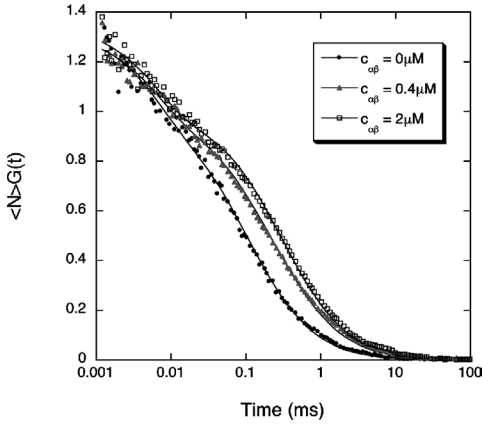

Fig. 3. Example of three autocorrelation curves measured for the fluorescent NLS peptide in the absence (black dots) or in the presence of an equimolar concentration $c_{\alpha\beta}$ of importin α and importin β, with either $c_{\alpha\beta} = 0.4$ mM (gray triangles) or $c_{\alpha\beta} = 2$ mM (empty squares). The lines are fit to Eq. (2), where the values $S = 6.4$, $\tau_T = 6$ μs, $\tau_{D,1} = 96$ μs and $\tau_{D,2} = 326$ μs have been fixed.

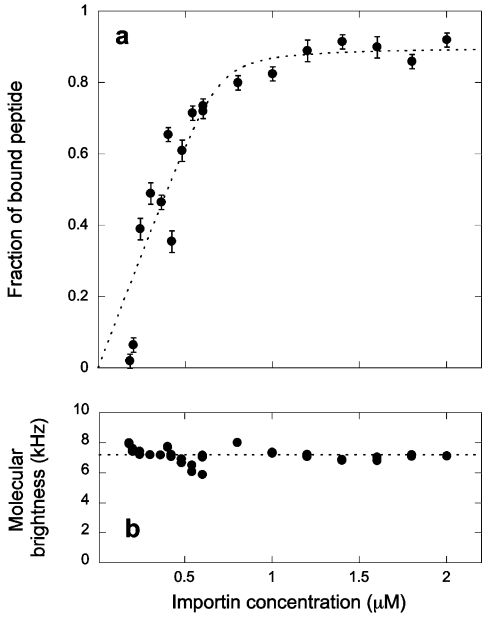

Fig. 4. (**a**) Titration curve showing the fraction of peptide bound to the complex formed by importin α and importin β and (**b**) apparent fluorescence per molecule calculated as explained in the text, as a function of the concentration $c_{\alpha\beta}$ of the complex. The dashed line in (**a**) represents a fit to a simple binding model (Eq. (7)), which gave $K_D = 12 \pm 3$ nM, $c_p = 700 \pm 100$ nM and $f_0 = 10\%$.

This indicates that the Alexa dye is not quenched when the peptide becomes part of a cargo complex and also that the quantity y shown in Fig. 4a is the actual fraction of peptides that are part of a cargo complex. In Fig. 4, the concentration $c_{\alpha\beta}$ of the importin α/β heterodimer was calculated assuming no protein was lost during the dilutions or because of adsorption on the glass.

Table 1

Peptide	Ligand	Dissociation constant K_D
Alexa-NLS	α/β heterodimer	12 ± 3 nM
Alexa-bNLS	α/β heterodimer	>100 nM
Alexa-NLS	Importin α	>1 μM
Alexa-NLS	α/β heterodimer, RanGDP present	2 ± 10 nM
Alexa-NLS	α/β heterodimer, RanGTP present	>1 μM
α/β heterodimer	RanGTP	<0.2 nM
Alexa-NLS/α/β heterodimer	RanGTP	18 ± 16 nM

The binding curve in Fig. 4a was analyzed using the simple binding model leading to Eq. (7). The fit of the data presented in Fig. 4a with this model gave $K_D = 12 \pm 3$ nM and $c_p = 700 \pm 100$ nM. The fraction of peptide unable to bind to the importin α/β heterodimer was in this case $f_0 = 10\%$. This fraction was found to depend a lot on the peptide sample used for assay, perhaps reflecting different purities.

To validate the result of this experiment, several different titrations were performed as controls. First we checked that the α/β complex was binding specifically to the NLS sequence of the Alexa-NLS peptide, by repeating the same titration using the Alexa-bNLS peptide. Although some evidence of binding at high importin concentration was detected, the dissociation constant K_D associated with this reaction is at least one order of magnitude larger for the bNLS peptide than for the NLS peptide. We also verified that no binding occurred in the absence of importin β, in which case we could detect only marginal binding of the peptide to importin α, with a dissociation constant K_D that from our experiment could be estimated to be at least two orders of magnitude larger than that in the presence of importin β. The different dissociation constants obtained are summarized in Table 1.

We next studied the dissociation of the cargo complex by RanGTP. For this, we titrated solutions containing a concentration $c_p = 50$ nM of the fluorescent peptide (as measured by FCS) and 2 μM of both importin α and importin β with increasing amounts of either RanGDP or RanGTP, up to a concentration $c_R = 4$ μM. The concentrations of importin α and β were chosen to be in large excess compared to the peptide concentration in order for all the NLS peptides to be part of a cargo complex in the absence of Ran. In this case, the total concentration of cargo complex in the absence of Ran is hence $c_{NLS\alpha\beta} = c_p \approx 50$ nM. The result of the titration is shown in Fig. 5. It is clear from the experiment that, while RanGDP has no visible effect on

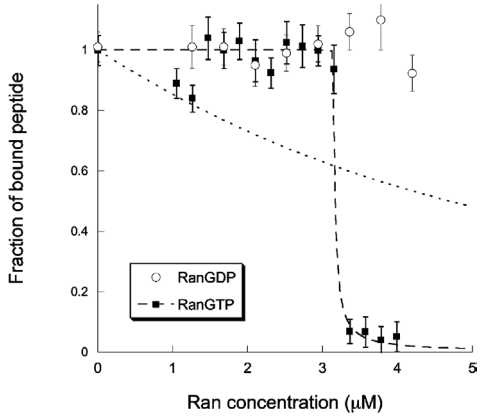

Fig. 5. Titration curves showing the fraction of Alexa-NLS bound to a cargo complex as a function of the introduced concentration of RanGTP (filled squares) or RanGDP (empty circles). The lines represent fits of the RanGTP titration curve using either Eq. (8) (dotted line) or Eq. (9) (dashed line). This second fit gives $K_D = 0 \pm 0.1$ nM and $K_D^{NLS} = 21 \pm 20$ nM.

the stability of the cargo complex, RanGTP is able to dissociate it. Most notably, the titration curve we obtain cannot be explained by a simple model where RanGTP binds without distinction the importin α/β heterodimer and the α/β/NLS cargo complexes. If this were the case, we would expect the fraction of free peptide (i.e. of peptide not bound to a cargo complex) to follow the trend captured in Eq. (8), but this model (dotted line in Fig. 5) does not account properly for the experimental result. Instead, we must allow for RanGTP to have a lower affinity for cargo complexes associated with a NLS peptide than for simple importin α/β heterodimers in order to explain our observations. To do so, we assume that the concentration of dissociated cargo complexes is always much smaller than the concentration of dissociated importin α/β heterodimers. This is a reasonable assumption since the total initial importin α/β heterodimer concentration, $c_{\alpha\beta} \approx 2$ μM, is an order of magnitude larger than the total initial cargo complex concentration, $c_{\mathrm{NLS}\alpha\beta} \approx 50$ nM. In that case, as explained in the § *Materials and methods*, the fraction of importin α/β heterodimers that have not yet been dissociated by Ran, $f_{\alpha\beta}$, obeys Eq. (8), while the fraction of cargo complexes which has not been dissociated by Ran, $f_{\mathrm{NLS}\alpha\beta}$, obeys Eq. (9). In the particular experiment shown in Fig. 5, the totality of the NLS peptides was initially bound to the α/β heterodimer, so there was no need to account for an unbound fraction. As can be seen in Fig. 5, this model (dashed line in Fig. 5) accounts very well for our observations. Up until $c_R \approx 3$ μM, the effect of RanGTP is to dissociate the free α/β heterodimers, to which RanGTP presumably binds with greater affinity, so that no dissociation of the cargo complexes containing the NLS peptide can be detected. For $c_R > 3$ μM, after most of the α/β heterodimers have been dissociated, we begin to observe dissociation of cargo complexes containing the NLS peptide. With this model, the dissociation constants extracted from the analysis indicate that the affinity of RanGTP for the free importin α/β heterodimer is significantly greater than for the α/β/NLS cargo complex. In the first case the associated dissociation constant is $K_D < 0.2$ nM, while it is $K_D^{NLS} = 18 \pm 16$ nM in the second case. No affinity of RanGDP for the cargo complex could be detected.

4. Discussion

Fluorescence correlation spectroscopy is a powerful method that allows detection of binding of fluorescent ligands to receptors directly in solution. The diffusion coefficient of the receptor just needs to be 1.6 times larger than that of the ligand [27]. Since FCS is very well suited for working with nanomolar concentrations of reactants, it should be an ideal method to measure interactions between biomolecules, for which binding is often very tight, with dissociation constants in the nM range. However, when trying to determine equilibrium constants for reactions involving soluble components, surface adsorption is a critical problem. It can severely reduce the concentration of the reactants in solution, introducing several unknown variables. In particular, the negative charge density of glass surfaces, acquired through the dissociation of silanol groups, is an issue for the study of small concentration of positively charged or hydrophobic peptides. We were able to alleviate this problem by using ovalbumin to crowd the solution. For the highly positively charged peptides we studied, an ovalbumin concentration of at least 1 g l^{-1} was required to begin to displace the peptides from the glass surfaces. At 5 g l^{-1}, the ovalbumin was able to compete efficiently against the peptide for surface adsorption, and above 10 g l^{-1} all the peptides were displaced from the surfaces. On the other hand, above a 5-g l^{-1} concentration of ovalbumin, we began to see an influence of the ovalbumin on the peptide diffusion, with a diffusion coefficient reduced by more than 10% at 10 g l^{-1}. This is probably due to an increase in the effective viscosity of the solution, though it is also possible that at these high concentrations the peptide starts to interact with the protein, or that inhomogeneities form in the solution due to depletion interactions. For this reason, we chose not to use ovalbumin concentration above 5 g l^{-1}. The fact that the molecular brightness of the fluorophore did not change when increasing the ovalbumin concentration

showed that up to 50 $g\,l^{-1}$ the optical index mismatch created by the addition of protein is not large enough to cause strong optical aberrations.

Because of adsorption on the sample chamber surfaces, the precision with which we could evaluate the concentration of the reactants, and consequently extract binding constants, proved to be limited. Relative measurements, on the other hand, should not be strongly affected by such uncertainties. While the peptide concentration in solution could be monitored through the FCS measurement, the concentration of the purified proteins (importin α, importin β, and Ran) had to be estimated. The fit to the data in Figs. 4a and 5 give sensible results only if the protein concentrations are allowed to float. This emphasizes the usefulness of cross-correlation spectroscopy, where the absolute concentration of both receptor and ligand can be monitored, and where there is no need for one reactant to be much larger in size than the other. Measurement of dissociation constants larger than 1 μM was problematic, as the concentration of ligand required in order to achieve full binding is higher than what could be obtained. In those cases, the values measured have a large uncertainty associated with them.

Our titration experiments are all in good agreement with the equilibrium constants measurements determined by other techniques [15,16,29]. For the interaction of the SV40 large T-antigen NLS with the importin α/β heterodimer, we measure a dissociation constant $K_D = 12 \pm 8$ nM. This is comparable to that measured by fluorescence depolarization for the same NLS fused to GFP interacting with a mutant importin α lacking the self-inhibitory domain, $K_D = 9 \pm 4$ nM, or with the importin α/β complex, $K_D = 33$ nM [16]. It is also very close to the value of the dissociation constant measured by biosensor analysis for the interaction between a NLS peptide similar to the one used in this study with either a mutant importin α lacking the self-inhibitory domain, $K_D = 15$ nM or with the importin α/β complex, $K_D = 35$ nM [15]. Similarly, the dissociation constant we estimate for the peptide containing the reversed sequence of the SV40 large T-antigen NLS, $K_D \approx 100$ nM, is within the range of dissociation constants measured for mutant SV40 large T-antigen NLS sequences tested by Hodel et al., found to vary from 16 nM to about 10 μM (although none of the sequences tested in that study was similar to ours) [29].

Overall, our experiments with RanGTP and RanGDP are also in agreement with the accepted model of nuclear transport, which is based on the notion that the gradient of RanGTP across the nuclear membrane drives vectorial transport by dissociating cargo complexes once they reach the nucleus. Our titration shows that indeed RanGTP is able to dissociate cargo complexes and to release the NLS carrying cargo, while RanGDP has no noticeable effect on the cargo complexes. Moreover, we show that RanGTP has a different affinity for importin β when it is part of a α/β heterodimer than when it is part of a NLS/α/β cargo complex. It has been assumed previously that the affinity of RanGTP for a complete cargo complex might be reduced about five times compared to its affinity for the α/β heterodimer alone [30]. Our measurements validate this hypothesis. Although the binding constants we measured should be taken as estimates rather than exact values, it emerges from the data presented in Fig. 5 that the affinity of RanGTP for importin β when part of an α/β heterodimer is at least 10 times larger than for importin β when it is part of a complete NLS/α/β cargo complex. The effect we observe may be due to a much tighter binding between importin α and importin β in presence of a NLS carrying cargo, making it more difficult for RanGTP to take advantage of transient conformational changes of the complex to bind to importin β. Indeed, the rate constant for dissociation of the α/β heterodimer has been measured to be as high as 0.02 s^{-1} [30], indicating that this complex might undergo structural fluctuations leading to conformational changes partially exposing the Ran binding domain of importin β. There is no information available about the dissociation rate of importin β from importin α when the latter is bound to a NLS. Our experiments could suggest that this rate constant is at least 10 times smaller than in the absence of the NLS sequence.

The fact that the dissociation of cargo complexes depends on whether or not they are actually loaded with a cargo might have interesting consequences in nucleocytoplasmic transport. It could mean that different cargoes, which bind to importin α with different affinities [29], will be dissociated by RanGTP in a different order. If the rate-limiting step for the import of a specific cargo is the dissociation of the cargo complex by RanGTP, then the kinetics of import might be very dependent on the type of NLS carried by the cargo. In the larger context of the role of the soluble nuclear import receptors as control proteins in various mitotic processes, the possibility of a preferential release of importin β when it binds to different targets is also quite interesting. It could explain how the very different molecular switch functions of the importin β/RanGTP pair may be orchestrated by the cell. It has been proposed that this difficult coordination could be achieved by the presence of other (still remaining to be identified) regulators of importin β, in addition to RanGTP [7]. However, both

importin β and RanGTP are very abundant, and it is unlikely that a new regulator of importin β, if it is discovered, could be as dominant as Ran. Our results suggest a different explanation, namely that RanGTP itself, through its preferential affinity for importin β when bound to specific cargoes, is able to regulate which targets of the importin α/β heterodimer it will release.

Acknowledgements

We thank Dr. D. Görlich and Dr. R. Nevo for providing us with purified proteins, and Dr. M. Peretz for expert technical assistance. This work was supported in part by a grant from the Israel Science Foundation – The Charles H. Revson Foundation, and by the Gerhardt M.J. Schmidt Minerva Center for Supramolecular Architecture. C.F. was supported partly by a Marie-Curie research fellowship, and partly by the Natural Sciences and Engineering Research Council of Canada through its CRC program.

References

[1] L.F. Pemberton, G. Blobel, J.S. Rosenblum, Transport routes through the nuclear pore complex, Curr. Opin. Cell Biol. 10 (1998) 392–399.
[2] D. Gorlich, U. Kutay, Transport between the cell nucleus and the cytoplasm, Annu. Rev. Cell Dev. Biol. 15 (1999) 607–660.
[3] S.A. Adam, Transport pathways of macromolecules between the nucleus and the cytoplasm, Curr. Opin. Cell Biol. 11 (1999) 402–406.
[4] R. Bayliss, A.H. Corbett, M. Stewart, The molecular mechanism of transport of macromolecules through nuclear pore complexes, Traffic 1 (2000) 448–456.
[5] M. Kunzler, E. Hurt, Targeting of Ran: variation on a common theme?, J. Cell Sci. 114 (2001) 3233–3241.
[6] P. Kalab, K. Weis, R. Heald, Visualization of a Ran-GTP gradient in interphase and mitotic Xenopus egg extracts, Science 295 (2002) 2452–2456.
[7] A. Harel, D.J. Forbes, Importin beta: conducting a much larger cellular symphony, Mol. Cell 16 (2004) 319–330.
[8] M.V. Nachury, T.J. Maresca, W.C. Salmon, C.M. Waterman-Storer, R. Heald, K. Weis, Importin β is a mitotic target of the small GTPase Ran in spindle assembly, Cell 104 (2001) 95–106.
[9] O.J. Gruss, C.A. Carazo-Salas, C.A. Schatz, G. Guargaglini, J. Kast, M. Wilm, N. Le Bot, I. Vernos, E. Karsenti, I.W. Mattaj, Ran induces spindle assembly by reversing the inhibitory effect of importin α on TPX2 activity, Cell 104 (2001) 89–93.
[10] C. Zhang, P.R. Clarke, Chromatin-independent nuclear envelope assembly induced by Ran GTPase in Xenopus egg extracts, Science 288 (2000) 1429–1432.
[11] C. Zhang, M.W. Goldberg, W.J. Moore, T.D. Allen, P.R. Clarke, Concentration of Ran on chromatin induces decondensation, nuclear envelope formation and nuclear pore complex assembly, Eur. J. Cell Biol. 81 (2002) 623–633.
[12] B. Di Fiore, M. Ciciarello, R. Mangiacasale, A. Palena, A.M. Tassin, E. Cundari, P. Lavia, Mammalian RanBP1 regulates centrosome cohesion during mitosis, J. Cell Sci. 116 (2003) 3399–3411.
[13] J.M. Casolari, C.R. Brown, S. Komili, J. West, H. Hieronymus, P.A. Silver, Genome-wide localization of the nuclear transport machinery couples transcriptional status and nuclear organization, Cell 117 (2004) 427–439.
[14] E. Conti, E. Izaurralde, Nucleocytoplasmic transport enters the atomic age, Curr. Opin. Cell Biol. 13 (2001) 310–319.
[15] B. Catimel, T. Teh, M.R. Fontes, I.G. Jennings, D.A. Jans, G.J. Howlett, E.C. Nice, B. Kobe, Biophysical characterization of interactions involving importin-alpha during nuclear import, J. Biol. Chem. 276 (2001) 34189–34198.
[16] P. Fanara, M. Hodel, A. Corbett, A. Hodel, Quantitative analysis of nuclear localization signal (NLS)-importin alpha interaction through fluorescence depolarization. Evidence for autoinhibitory regulation of NLS binding, J. Biol. Chem. 275 (2000) 21218–21223.
[17] D. Gorlich, S. Kostka, R. Kraft, C. Dingwall, R.A. Laskey, E. Hartmann, S. Prehn, Two different subunits of importin cooperate to recognize nuclear localization signals and bind them to the nuclear envelope, Curr. Biol. 5 (1995) 383–392.
[18] N. Imamoto, T. Tachibana, M. Matsubae, Y. Yoneda, A karyophilic protein forms a stable complex with cytoplasmic components prior to nuclear pore binding, J. Biol. Chem. 270 (1995) 8559–8565.
[19] W. Webb, Fluorescence correlation spectroscopy: inception, biophysical experimentations, and prospectus, Appl. Opt. 40 (2001) 3969–3983.
[20] M.A. Medina, P. Schwille, Fluorescence correlation spectroscopy for the detection and study of single molecules in biology, Bioessays 24 (2002) 758–764.
[21] R. Rigler, U. Mets, J. Widengren, P. Kask, Fluorescence correlation spectroscopy with high count rate and low background: analysis of translational diffusion, Eur. Biophys. J. 22 (1993) 169–175.
[22] J. Widengren, R. Rigler, Fluorescence correlation spectroscopy as a tool to investigate chemical reactions in solutions and on cell surfaces, Cell Mol. Biol. (Noisy-le-Grand) 44 (1998) 857–879.
[23] C. Klebe, F.R. Bischoff, H. Ponstingl, A. Wittinghofer, Interaction of the nuclear GTP-binding protein Ran with its regulatory proteins RCC1 and RanGAP1, Biochemistry 34 (1995) 639–647.
[24] R. Nevo, C. Stroh, F. Kienberger, D. Kaftan, V. Brumfeld, M. Elbaum, Z. Reich, P. Hinterdorfer, A molecular switch between alternative conformational states in the complex of Ran and importin beta1, Nat. Struct. Biol. 10 (2003) 553–557.
[25] C. Fradin, A. Abu-Arish, R. Granek, M. Elbaum, Fluorescence correlation spectroscopy close to a fluctuating membrane, Biophys. J. 84 (2003) 2005–2020.
[26] J. Widengren, U. Mets, R. Rigler, Fluorescence correlation spectroscopy of triplet states in solution: a theoretical and experimental study, J. Phys. Chem. 99 (1995) 13368–13379.
[27] D. Magde, E.L. Elson, W.W. Webb, Fluorescence correlation spectroscopy. II. An experimental realization, Biopolymers 13 (1974) 29–61.
[28] R. Brock, T. Jovin, Fluorescence correlation microscopy: Fluorescence correlation spectroscopy in cell biology, in: R. Rigler, E. Elson (Eds.), Fluorescence Correlation Spectroscopy, Theory and Application, Springer, 2001, pp. 132–161.
[29] M. Hodel, A. Corbett, A. Hodel, Dissection of a nuclear localization signal, J. Biol. Chem. 276 (2001) 1317–1325.
[30] G. Riddick, I.G. Macara, A systems analysis of importin-α–β mediated nuclear protein import, J. Cell Biol. 168 (2005) 1027–1038.